Heinrich Heine
Universität
Düsseldorf

Molecular characterization of the CXCR4 / CXCR7 axis in germ cell tumors and its targetability using nanobody-drug-conjugates

Gamal A. Wakileh, Philipp Bierholz, Mara Kotthoff, Margaretha A. Skowron, Felix Bremmer, Alexa Stephan, Stephanie M. Anbuhl, Raimond Heukers, Martine J. Smit, Philipp Ströbel, Daniel Nettersheim

Article - Version of Record

Suggested Citation:
Wakileh, G. A., Bierholz, P., Kotthoff, M., Skowron, M. A., Bremmer, F., Stephan, A., Anbuhl, S. M., Heukers, R., Smit, M. J., Ströbel, P., & Nettersheim, D. (2023). Molecular characterization of the CXCR4 / CXCR7 axis in germ cell tumors and its targetability using nanobody-drug-conjugates. Experimental Hematology & Oncology, 12, Article 96. https://doi.org/10.1186/s40164-023-00460-9

Wissen, wo das Wissen ist.

UNIVERSITÄTS- UND LANDESBIBLIOTHEK DÜSSELDORF

This version is available at:

URN: https://nbn-resolving.org/urn:nbn:de:hbz:061-20241030-112406-5

Terms of Use:

This work is licensed under the Creative Commons Attribution 4.0 International License.

For more information see: https://creativecommons.org/licenses/by/4.0

Experimental Hematology & Oncology

CORRESPONDENCE

Open Access

Molecular characterization of the CXCR4 / CXCR7 axis in germ cell tumors and its targetability using nanobody-drug-conjugates

Gamal A. Wakileh[1,2], Philipp Bierholz[1,6], Mara Kotthoff[1,6], Margaretha A. Skowron[1,6], Felix Bremmer[3], Alexa Stephan[1,6], Stephanie M. Anbuhl[4,5], Raimond Heukers[4,5], Martine J. Smit[4], Philipp Ströbel[3] and Daniel Nettersheim[1,6*]

Abstract

Being stimulated by the chemokine CXCL12, the CXCR4 / CXCR7 cascade is involved in tumor proliferation, migration, and metastasis. The interaction between CXCL12, secreted by cells from the microenvironment, and its receptors is complex and has been ascribed to promote chemotherapy resistance. However, the role of this signaling axis and its targetability in germ cell tumors (GCT) is not fully understood. Thus, this study investigated the therapeutic efficacy of a nanobody-drug-conjugate targeting CXCR4 (CXCR4-NDC) and functionally characterized this signaling pathway in GCT using small molecule inhibitors and nanobodies. As shown by diminished cell viability, enhanced apoptosis induction, and detection of mitotic catastrophes, we confirmed the cytotoxic efficacy of the CXCR4-NDC in $CXCR4^{+}$-GCT cells (i.e. seminoma and yolk-sac tumor), while non-malignant $CXCR4^{-}$-fibroblasts, remained largely unaffected. Stimulation of $CXCR4^{+}$ / $CXCR7^{+}$-GCT cells with CXCL12 resulted in an enhanced proliferative and migratory capacity, while this effect could be reverted using CXCR4 inhibitors or a CXCR7-nanobody. Molecularly, the CXCR4 / CXCR7-signaling cascade could be activated independently of MAPK (ERK1 / 2)-phosphorylation. Although, in $CXCR4^{-}$ / $CXCR7^{-}$-embryonal carcinoma cells, *CXCR7*-expression was re-induced upon inhibition of ERK1 / 2-signaling. This study identified a nanobody-drug-conjugate targeting CXCR4 as a putative therapeutic option for GCT, i.e. seminoma and yolk-sac tumors. Furthermore, this study shed light on the functional role of the CXCR4 / CXCR7 / CXCL12-signaling cascade in GCT, demonstrating an important influence on proliferation and migration.

Keywords Germ cell tumors, Testis cancer, Therapy, Resistance, Nanobody-drug-conjugate, CXCR4, CXCR7, CXCL12

*Correspondence:
Daniel Nettersheim
Daniel.Nettersheim@med.uni-duesseldorf.de
[1]Department of Urology, Urological Research Laboratory, Translational UroOncology, Medical Faculty and University Hospital Düsseldorf, Heinrich Heine University Düsseldorf, Moorenstraße 5, 40225 Düsseldorf, Germany
[2]Department of Urology, University Hospital Ulm, Ulm, Germany
[3]Institute of Pathology, University Medical Center Göttingen, Göttingen, Germany
[4]Amsterdam Institute for Molecular and Life Sciences, Division of Medicinal Chemistry, Faculty of Sciences, Vrije Universiteit, Amsterdam, Netherlands
[5]QVQ Holding BV, Utrecht, the Netherlands
[6]Center for Integrated Oncology Aachen Bonn Cologne Düsseldorf (CIO ABCD), Düsseldorf, Germany

© The Author(s) 2023. **Open Access** This article is licensed under a Creative Commons Attribution 4.0 International License, which permits use, sharing, adaptation, distribution and reproduction in any medium or format, as long as you give appropriate credit to the original author(s) and the source, provide a link to the Creative Commons licence, and indicate if changes were made. The images or other third party material in this article are included in the article's Creative Commons licence, unless indicated otherwise in a credit line to the material. If material is not included in the article's Creative Commons licence and your intended use is not permitted by statutory regulation or exceeds the permitted use, you will need to obtain permission directly from the copyright holder. To view a copy of this licence, visit http://creativecommons.org/licenses/by/4.0/. The Creative Commons Public Domain Dedication waiver (http://creativecommons.org/publicdomain/zero/1.0/) applies to the data made available in this article, unless otherwise stated in a credit line to the data.

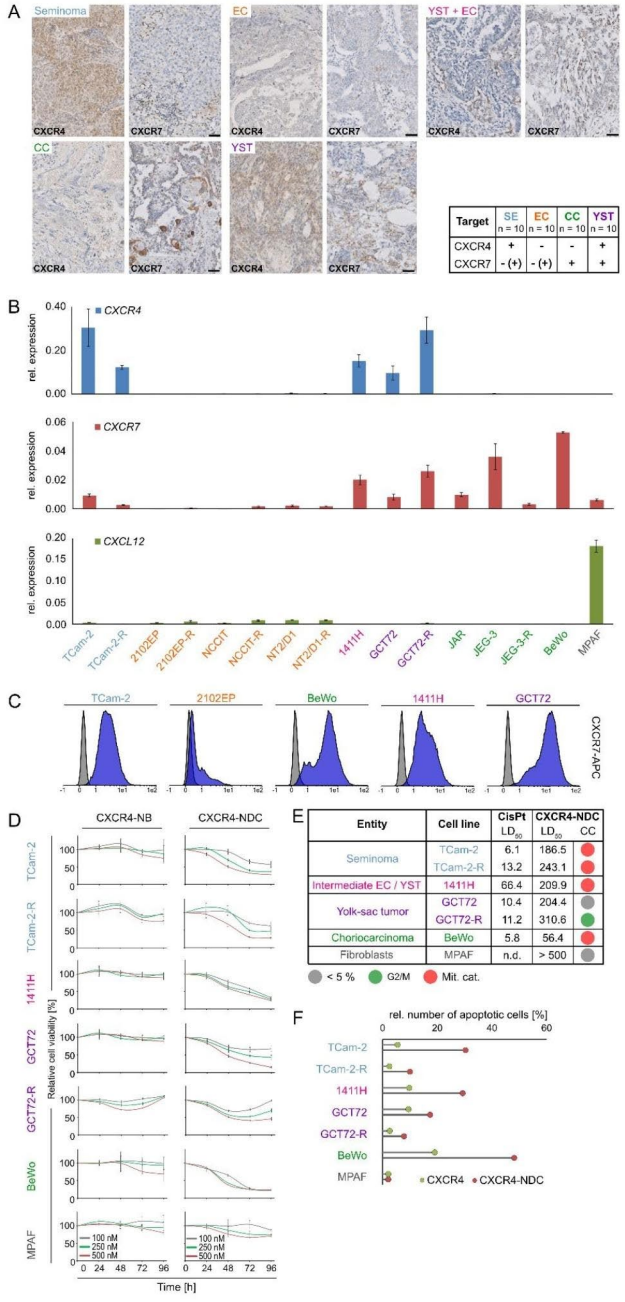

Fig. 1 (**A**) Immunohistochemical evaluation of CXCR4 / CXCR7 in SEM, CC, YST and YST + EC mixed GCT. (**B**) Relative expression of *CXCR4*, *CXCR7*, and *CXCL12* in GCT cell lines and fibroblasts (MPAF). *ACTB* and *GAPDH* were used as housekeeping genes. (**C**) Flow cytometry data of CXCR7-APC stained GCT cell lines (blue) compared with unstained controls (grey). (**D**) XTT cell viability assays of GCT cell lines and fibroblasts (MPAF) treated with CXCR4-NDC or CXCR4-NB alone for 24–96 h. (**E**) LD_{50} values measured by XTT cell viability assays 72 h after treatment with cisplatin (CisPt, µM) or CXCR4-NDC (nM) and color-coded changes in cell cycle distribution (mitotic catastrophe = red; changes < 5% = grey) upon treatment with CXCR4-NDC (LD_{50} concentrations) for 72 h as compared to the CXCR4-NB alone. (**F**) Lollipop graph summarizing the relative number of apoptotic cells in $CXCR4^+$ GCT cells and $CXCR4^-$ MPAF upon treatment with either CXCR4-NDC or CXCR4-NB alone (LD_{50} concentrations) for 72 h

To the editor

GCT account for 1–2% of all neoplasms occurring in the male population, but represent the most common cancer type in young men [1]. The CXCR4 / CXCR7 / CXCL12-cascade has been postulated to play a major role during metastasis in GCT. In this study, we therapeutically targeted this axis in GCT. Further, we characterized the molecular role of this cascade.

According to 'The Cancer Genome Atlas' (TCGA), mutations in *CXCR4* / *CXCR7* were not found in GCT (Fig. S1A). On protein level, seminoma (SEM) tissues presented as $CXCR4^+$/ $CXCR7^-$, embryonal carcinoma (EC) as $CXCR4^-$ / $CXCR7^-$, choriocarcinoma (CC) as $CXCR4^-$ / $CXCR7^+$, and yolk-sac tumors (YST) as $CXCR4^+$ / $CXCR7^+$ (Fig. 1A). In mixed GCT (YST + EC), only YST cells were $CXCR4^+$ / $CXCR7^+$. In GCT cell lines including cisplatin-resistant subclones (-R), similar observations were found on mRNA level (SEM: TCam-$2^{CXCR4+/CXCR7+}$; EC: 2102EP / NT2/D1 / $NCCIT^{CXCR4-/CXCR7-}$; CC: JAR / JEG-3 / $BeWo^{CXCR4-/CXCR7+}$; YST: $GCT72^{CXCR4+/CXCR7+}$; intermediate EC / YST: $1411H^{CXCR4+/CXCR7+}$) (Fig. 1B; Fig. S1B). *CXCR7* expression profiles could be confirmed on protein level (Fig. 1C). Previously, on protein level we already demonstrated that SEM and YST cells present as $CXCR4^+$, while EC and CC cells were $CXCR4^-$ [2]. Fibroblasts (MPAF) showed negligible *CXCR4* / *CXCR7* levels, while expressing and secreting CXCL12 (Fig. 1B; Fig. S1C).

We therapeutically targeted CXCR4 by a nanobody coupled to the spindle-toxin monomethyl-auristatin-E (nanobody-drug-conjugate; NDC) [3]. Treatment of SEM and YST cells with the CXCR4-NDC decreased cell viability compared to the uncoupled CXCR4-nanobody (CXCR4-NB) (Fig. 1D, E). The LD_{50} concentrations for the CXCR4-NDC were between 56.4 and 310.6 nM for GCT cells (including cisplatin-resistant sub clones (-R)) and > 500 nM for fibroblasts, thereby opening a therapeutic window (Fig. 1E). A CXCR4-NDC treatment mainly resulted in mitotic catastrophes (TCam-2 / -R, 1411H, BeWo) and induction of apoptosis in $CXCR4^+$-cells (Fig. 1E, F; Fig. S1D). In fibroblasts, the cell cycle and apoptosis remained unaffected (Fig. 1E, F; Fig. S1D).

Next, we deciphered the molecular role of this signaling axis on mRNA and phospho-proteome level. Treatment with recombinant CXCL12 (100 ng / ml, 8 h) resulted in enhanced levels of *FOS* and *MMP3* in $GCT72^{CXCR4+/CXCR7+}$ and $BeWo^{CXCR7+}$ cells, while BeWo cells further showed increased expression of *CD44*, *IL6*, *ITGA4A*, and *MMP1* (Fig. S1E). Further, phospho-kinase-arrays were performed in $CXCR4^+$ / $CXCR7^+$ cells 24 h after treatment with recombinant CXCL12 (250 ng / ml) (Fig. 2A; Fig. S1F). In TCam-2^{CXCR4+} we found increased phosphorylation (p-) of β-Catenin and STAT5a / b

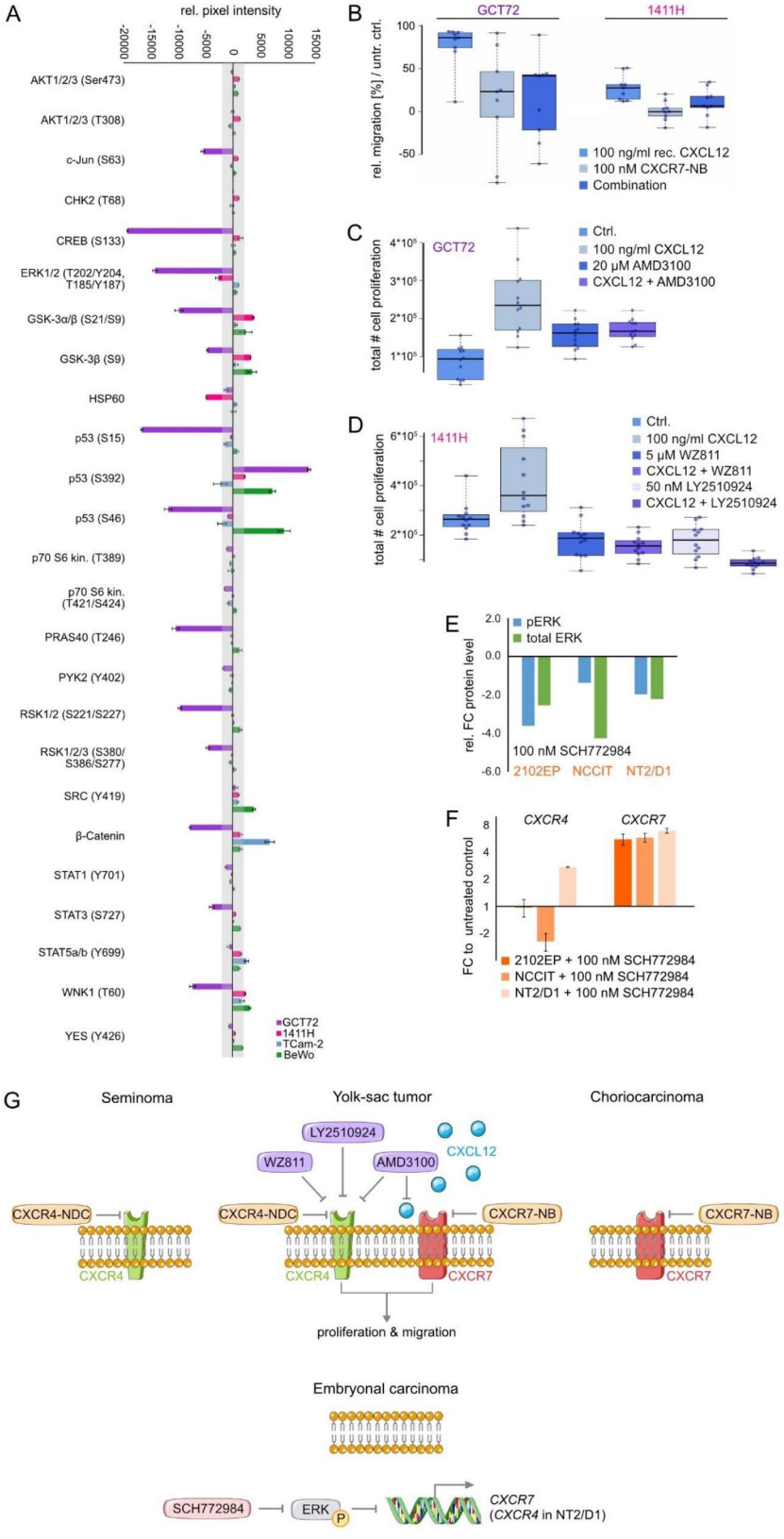

Fig. 2 (See legend on next page.)

(See figure on previous page.)

Fig. 2 (**A**) Densitometric evaluation of relative pixel intensities (normalized to untreated controls) of the indicated phosphorylation sites in cell lysates from GCT72, 1411H, TCam-2 and BeWo cells treated with recombinant CXCL12 (250 ng / ml) for 24 h, as measured by a human phospho-kinase array. (**B**) Relative migration of GCT72 and 1411H cells treated with either 100 ng / ml recombinant CXCL12, 100 nM CXCR7-NB (VUN702), or the combination of both, in comparison with the untreated control. (**C**) Box plot summarizing the number of proliferative GCT72 cells treated with 100 ng / ml recombinant CXCL12, 20 µM CXCR4-inhibitor AMD3100, or the combination of both for 24 h in comparison to the untreated control. (**D**) Box plot summarizing the number of proliferative 1411H cells treated with 100 ng / ml recombinant CXCL12, CXCR4-inhibitors WZ811 (5 µM) / LY2510924 (50 nM), or the combination of both for 32 h in comparison to the untreated control. (**E**) Densitometric evaluation of western blot data of phospho- and total-ERK in EC cells (2102EP, NCCIT, NT2/D1) treated daily with 100 nM ERK inhibitor SCH772984 for 96 h. (**F**) Relative mRNA expression of *CXCR4* and *CXCR7* in EC cell lines (2102EP, NCCIT, NT2/D1) treated daily with 100 nM SCH772984 for 96 h as compared to untreated controls. *ACTB* and *GAPDH* were used as housekeeping genes. (**G**) Model summarizing key findings related to the CXCR4 / CXCR7 / CXCL12 axis. SEM present as $CXCR4^+$ / $CXCR7^-$, YST as $CXCR4^+$ / $CXCR7^+$, CC as $CXCR4^-$ / $CXCR7^+$ and EC as $CXCR4^-$ / $CXCR7^-$. SEM (also with occult YST subpopulations), YST and CC are targetable by CXCR4- and / or CXCR7-NDC, respectively. CXCL12 stimulated CXCR4 / CXCR7 enhanced proliferation and migration in YST cells. In EC cell lines, inhibition of MAPK (ERK1 / 2) signaling allows for re-induction of *CXCR7* expression (and partly *CXCR4*)

(Y699), in $1411H^{CXCR4+/CXCR7+}$ elevated p-GSK-3α / β (S21 / S9), p-p53 (S392) and p-WNK1 (T60), and in $BeWo^{CXCR7+}$ enhanced levels of p-GSK-3α / β (S21 / S9), p-p53 (S392 / S46), p-SRC (Y419) and p-WNK1 (T60). In $GCT72^{CXCR4+/CXCR7+}$ cells, phosphorylation of thirteen signaling-molecules, including ERK1 / 2 (T202 / Y204, T185 / Y187), GSK-3α / β (S21 / S9), β-Catenin, and p53 (S15 / S46) was reduced, while p-p53 (S392) was strongly enhanced. Phosphorylation of p53 at S15 has been described to increase stability of p53 by blocking MDM2 binding [4, 5]. Similarly, phosphorylation of S392 is also known to stabilize p53, influence its mitochondrial translocation and a transcription-independent apoptotic function. At a later time-point of DNA damage, S46 phosphorylation initiates the p53-mediated apoptosis through the induction of pro-apoptotic genes, such as *p53AIP1* [4, 5]. Hence, in CXCL12-stimulated BeWo cells, p53 phosphorylation at S15 and S46 might indicate an enhanced and stabilized pro-apoptotic p53 signaling cascade. Vice versa, CXCL12-stimulated GCT72 cells revealed a contrary phosphorylation pattern with diminished S15 and S46 phosphorylation of p53. Generally, the basal phosphorylation of all three evaluated p-p53 sites, particularly S46 and S392, is significantly higher in BeWo cells as compared to GCT72 (Fig. S1F), thereby indicating a more profound apoptosis signaling in BeWo cells upon treatment with the CXCR4-NDC (Fig. 1E, F). Thus, reduced p-p53-S15 / S46 after CXCL12-stimulation might diminish the activity of the apoptotic cascade in YST cells, thereby contributing to the high resistance of YST cells to cisplatin.

Furthermore, the migratory and proliferative capacity of $GCT72^{CXCR4+/CXCR7+}$ and $1411H^{CXCR4+/CXCR7+}$ cells was enhanced upon CXCL12-stimulation; this effect could be blocked upon application of a CXCR7-blocking nanobody (CXCR7-NB) or CXCR4-inhibitors (AMD3100, WZ811, LY2510924) (Fig. 2B-D, G). The CXCR4 / CXCR7-function after CXCL12 stimulation might also be mediated by receptor-heterodimerization [6, 7]. In YST $^{CXCR4+/CXCR7+}$ cells, we observed that blocking CXCR4 / CXCR7, abolished the effects on proliferation and migration, suggesting that both receptors act in concert to mediate their molecular functions.

We noted a discrepancy between a described CXCL12-dependent MAPK activation and our observed decreased MAPK signaling in CXCL12-stimulated cells [8–10]. Thus, we questioned, if ERK1 / 2 inhibition would influence *CXCR4* / *CXCR7* expression in $EC^{CXCR4-/CXCR7-}$ cells. Indeed, the ERK1 / 2 inhibitor SCH772984 decreased levels of total- and p-ERK1 / 2 (T202 / Y204-T185 / Y187), while increasing *CXCR7* expression (and *CXCR4* in NT2/D1) (Fig. 2E, F; Fig. S1F). Thus, in EC cells, *CXCR7* expression seems to be suppressed by MAPK-signaling, while in YST, diminished MAPK signaling after CXCL12 stimulation seems to allow for *CXCR7* expression (Fig. 2G).

In summary, we highlighted the CXCR4-NDC as a therapeutic option for $CXCR4^+$ SEM and YST (Fig. 2G). In YST and CC, also CXCR7 is a putative target, since an uncoupled CXCR7-NB was able to block the CXCR7-mediated molecular effects and proved to be functional. Thus, using a combination of CXCR4- and CXCR7-NDC could be advantageous for the treatment of mixed GCT consisting of SEM, YST and CC. The ability to target YST is of paramount interest, since YST represent the most aggressive GCT entity responsible for a majority of GCT-related death. Under chemotherapy, development of YST represents an escape mechanism, resulting in therapy-resistant relapses. Additionally, about 5% of metastatic SEM present as aggressive relapses accompanied by elevated AFP level, pointing at a YST-subpopulation [11]. In this setting, using a CXCR4-NDC would be beneficial to target both, SEM and the occult YST cells, by rendering the therapy more efficient and reducing the risk of a relapse. Due to tumor heterogeneity, the clinical need to explore tumor subtype-specific targets remains. As such, we identified CD24 to be a specific target for the treatment of EC using NK-CD24-CAR cells [12]. Moreover, we identified the tight-junction molecule CLDN6 as a putative target for the treatment of SEM, EC, CC, and partly YST by using a CLDN6-antibody-drug-conjugate [13]. As such, depending on the tumor subtype, a combined (immuno)therapeutic option should be considered for the treatment of heterogeneous tumors.

List of abbreviations

ABTS	2,2'-azino-bis(3-ethylbenzothiazoline-6-sulfonic acid
ADC	Antibody-drug-conjugate
CC	Choriocarcinoma
EC	Embryonal carcinoma
ELISA	Enzyme-linked immunosorbent assay
FFPE	Formalin-fixed, paraffin-embedded
GCT	Germ cell tumor
h	hour
LD_{50}	Lethal dose, 50%
min	minutes
MMAE	Monomethyl auristatin E
NB	Nanobody
NDC	Nanobody
NB	Nanobody-drug conjugate
nonSEM	Non-seminoma
p-	Phosphorylation
PCA	Principal component analysis
RPKM	Reads per kilobase million
SEM	Seminoma
TCGA	The Cancer Genome Atlas
YST	Yolk-sac tumor
XTT	2,3-bis-(2-methoxy-4-nitro-5-sulfophenyl)-2 H-tetrazolium-5-carboxanilide

Supplementary Information

The online version contains supplementary material available at https://doi.org/10.1186/s40164-023-00460-9.

Supplementary Material 1: Fig. S1: A) Mutational status and mRNA expression profile of *CXCR4*, and *CXCR7* / *ACKR3* in the GCT-TCGA cohort. B) Expression profile (RPKM) of *CXCR4* / *CXCR7* in GCT cells based on previously published RNA sequencing data (GSE189472, GSE190792, GSE190022, GSE168646, and GSE195794). C) CXCL12-ELISA of supernatants from fibroblasts (MPAF) and GCT cells NCCIT and JAR. D) Flow cytometry data indicating changes in the cell cycle distribution of GCT cell lines and MPAF treated with the CXCR4-NBC (blue) in comparison to CXCR4-NB controls (grey). E) Expression of *BCL2*, *CD44*, *CD-L3A1*, *CCND1*, *EGFR*, *FOS*, *IL6*, *ITGA4*, *MMP1/2/3*, *SRC*, *TGFB1/2/3*, *VEGFA* in CXCL12-stimulated (100 ng / ml, 8 h) GCT72, 1411H, TCam-2, and BeWo cells as compared to their respective untreated controls. F) Raw data of a human phospho-kinase array of various cell lysates (GCT72, 1411H, TCam-2, BeWo) treated with recombinant CXCL12 (250 ng / ml) for 24 h. Untreated cells served as controls. G) Western blot analyses of pERK and total ERK of EC cells (2102EP, NCCIT, NT2/D1) treated daily with 100 nM ERK inhibitor SCH772984 for 96 h

Supplementary Material 2: Supplemental 'Material & Methods'

Supplementary Material 3: Table S1: A) cell lines, B) drugs, C) antibodies, and D) oligonucleotides used in this study

Acknowledgements

We kindly thank Anna Pehlke and Olga Dschun for excellent technical assistance. We would like to thank Prof. Dr. Michal Mego, PD Dr. Michael Peitz, Dr. Christoph Oing, Dr. Thomas Müller, Dr Janet Shipley, and Dr. Matthew Murray for providing cell lines and healthy control cells (see Table S1 A for affiliations and provided cell lines).

Author Contributions

Conception and design: DN Acquisition of data: GAW, PB, MK, MAS, FB, AS Analysis and interpretation of data: GAW, PB, MK, MAS, FB, DN Visualization: MAS, DN Drafting of the manuscript: MAS, MK, DN Critical revision of the manuscript: FB, PS, RH, MJS Statistical analysis: GAW, PB, MK, MAS, FB, DN Obtaining funding: DN, FB Administrative, technical, or material support: FB, SA, RH, MJS, PS Supervision: DN.

Funding

D. Nettersheim was supported by the 'Deutsche Forschungsgemeinschaft' (NE 1861/8-1). F. Bremmer was supported by the 'Wilhelm Sander-Stiftung' (2016.041.1 /.2 /.3). G. A. Wakileh supported this study during his 'Ferdinand Eisenberger' research scholarship funded by the 'Deutsche Gesellschaft für Urologie' (DGU).

Data Availability

All data generated or analyzed during this study are included in this published article and its supplementary information files.

Declarations

Ethics approval and consent to participate

The ethics committee of the Heinrich Heine University Düsseldorf (HHU-D) raised no concerns on utilizing cell lines for in vitro experiments (vote 2018 – 178 to D. N.). The ethics committees of the HHU-D and the University Medical Center Göttingen (UMG) raised no concerns on performing the described experiments on GCT tissues from local biobanks (vote 2020.1247(_1) to D. N.; vote 20/09/20 to F. B., vote 24/4/20 to P. S.).

Consent for publication

All authors are aware of this article and agreed on publication.

Competing interests

The authors declare no competing interests.

Received: 24 January 2023 / Accepted: 17 November 2023
Published online: 23 November 2023

References

1. Znaor A, Lortet-Tieulent J, Jemal A, Bray F. International variations and trends in testicular cancer incidence and mortality. Eur Urol. 2014;65(6):1095–106.
2. Skowron MA, Becker TK, Kurz L, Jostes S, Bremmer F, Fronhoffs F, et al. The signal transducer CD24 suppresses the germ cell program and promotes an ectodermal rather than mesodermal cell fate in embryonal carcinomas. Mol Oncol. 2021;16(4):982–1008.
3. Johansson MP, Maaheimo H, Ekholm FS. New insight on the structural features of the cytotoxic auristatins MMAE and MMAF revealed by combined NMR spectroscopy and quantum chemical modelling. Sci Rep. 2017;7(1):15920.
4. Liu Y, Tavana O, Gu W. p53 modifications: exquisite decorations of the powerful guardian. J Mol Cell Biol. 2019;11(7):564–77.
5. Dai C, Gu W. p53 post-translational modification: deregulated in tumorigenesis. Trends Mol Med. 2010;16(11):528–36.
6. Koch C, Engele J. Functions of the CXCL12 receptor ACKR3/CXCR7-What has been Perceived and what has been overlooked. Mol Pharmacol. 2020;98(5):577–85.
7. Levoye A, Balabanian K, Baleux F, Bachelerie F, Lagane B. CXCR7 heterodimerizes with CXCR4 and regulates CXCL12-mediated G protein signaling. Blood. 2009;113(24):6085–93.
8. Santagata S, Ieranò C, Trotta AM, Capiluongo A, Auletta F, Guardascione G, et al. CXCR4 and CXCR7 signaling pathways: a focus on the Cross-talk between Cancer cells and Tumor Microenvironment. Front Oncol. 2021;11:591386.
9. Shi Y, Riese DJ, Shen J. The role of the CXCL12/CXCR4/CXCR7 Chemokine Axis in Cancer. Front Pharmacol. 2020;11:574667.
10. Huynh C, Dingemanse J, Meyer zu Schwabedissen HE, Sidharta PN. Relevance of the CXCR4/CXCR7-CXCL12 axis and its effect in pathophysiological conditions. Pharmacol Res. 2020;161:105092.
11. Wruck W, Bremmer F, Kotthoff M, Fichtner A, Skowron MA, Schönberger S, et al. The pioneer and differentiation factor FOXA2 is a key driver of yolk-sac tumour formation and a new biomarker for paediatric and adult yolk-sac tumours. J Cell Mol Med. 2021;25(3):1394–405.
12. Söhngen C, Thomas DJ, Skowron MA, Bremmer F, Eckstein M, Stefanski A, et al. CD24 targeting with NK-CAR immunotherapy in testis, prostate, renal and (luminal-type) Bladder cancer and identification of direct CD24 interaction partners. FEBS J. 2023;290(20):4864–876.
13. Skowron MA, Kotthoff M, Bremmer F, Ruhnke K, Parmaksiz F, Richter A, et al. Targeting CLDN6 in germ cell tumors by an antibody-drug-conjugate and studying therapy resistance of yolk-sac tumors to identify and screen specific therapeutic options. Mol Med. 2023;29(1):40.

Publisher's Note

Springer Nature remains neutral with regard to jurisdictional claims in published maps and institutional affiliations.